Magnetic properties of $Co_cNi_{1-c}Cl_2$-$FeCl_3$ graphite bi-intercalation compounds

Itsuko S. Suzuki, Catherine Vartuli, Charles R. Burr, and Masatsugu Suzuki
Department of Physics, State University of New York at Binghamton, Binghamton, New York 13902-6000
(Received 25 April 1994; revised manuscript received 20 June 1994)

$Co_cNi_{1-c}Cl_2$-$FeCl_3$ graphite bi-intercalation compounds (GBIC's) with the stacking sequence -G-$Co_cNi_{1-c}Cl_2$-G-$FeCl_3$-G- along the c axis have been prepared by a method of sequential intercalation. The intraplanar exchange interaction in $Co_cNi_{1-c}Cl_2$ layers is ferromagnetic, while the intraplanar exchange interaction in $FeCl_3$ layers is antiferromagnetic. The magnetic properties of $Co_cNi_{1-c}Cl_2$-$FeCl_3$ GBIC's have been studied by using dc and ac magnetic susceptibility, and low- and high-field SQUID magnetization meaurements. The $Co_cNi_{1-c}Cl_2$ layer undergoes a magnetic phase transition at the critical temperature T_c which changes from 19.48 K at $c=0$ to 9.10 K at $c=1$. A cluster glass phase appears below T_c where the spin directions of ferromagnetic clusters are frozen because of frustrated interisland interactions. Due to the intervening $FeCl_3$ layer the critical behavior of $Co_cNi_{1-c}Cl_2$-$FeCl_3$ GBIC's at T_c is three dimensional rather than two dimensional. Below T_N (≈ 4 K) the cluster glass phase may coexist with an antiferromagnetic long-range order occurring in the $FeCl_3$ layers. The effect of antiferromagnetic interplanar interaction between the $FeCl_3$ layer and the $Co_cNi_{1-c}Cl_2$ layer is clearly seen in the magnetization of $Co_cNi_{1-c}Cl_2$-$FeCl_3$ GBIC's. The nature of the coexisting phase is complicated by the spin frustration effect arising from the competition between the interplanar interaction between $FeCl_3$ and $Co_cNi_{1-c}Cl_2$ layers and the antiferromagnetic intraplanar interaction in the $FeCl_3$ layer.

I. INTRODUCTION

Recently the magnetic properties of magnetic ternary graphite intercalation compounds (TGIC's) have received considerable attention.[1-3] In these compounds two kinds of magnetic species are intercalated into galleries between graphite layers. Magnetic TGIC's include the magnetic random-mixture graphite intercalation compounds (RMGIC's) and graphite bi-intercalation compounds (GBIC's). The magnetic RMGIC's have magnetic intercalate layers which are formed of a random mixture of two kinds of magnetic species. Such magnetic RMGIC's include stage-2 $Co_cNi_{1-c}Cl_2$ GIC's,[4-6] stage-2 $Co_cMn_{1-c}Cl_2$ GIC's,[7,8] stage-2 $Ni_cMn_{1-c}Cl_2$ GIC's,[9] and stage-2 $Cu_cCo_{1-c}Cl_2$ GIC's:[10] Note that stage-2 $Co_cMg_{1-c}Cl_2$ GIC's (Refs. 11 and 12) do not belong to this category of magnetic RMGIC's because Mg^{2+} is a nonmagnetic ion. Due to the long c-axis repeat distance in stage-2 magnetic RMGIC's the interplanar exchange interaction between adjacent magnetic intercalate layers is much weaker than the intraplanar exchange interaction. Recent studies on the magnetic properties of these magnetic RMGIC's have proved that they provide the model systems for studying the magnetic phase transitions of two-dimensional (2D) random-spin systems with a spin-frustration effect arising from the competing spin anisotropy between XY and Heisenberg symmetry, and the competing intraplanar ferromagnetic and antiferromagnetic interactions.

The magnetic GBIC's offer possibilities for the formation of superlattices such as two different magnetic intercalate layers separated by a single graphite layer.[13-18] The magnetic GBIC can be synthesizes by the method of sequential intercalation. The intercalant I_2 is intercalated into empty graphite galleries of stage-2 I_1 GIC. The GBIC has a stacking sequence of $Gl_1Gl_2Gl_1Gl_2\ldots$ along the c axis, where two different intercalate layers (I_1 and I_2) alternate with a single graphite layer (G). The GBIC forms an ideal heterostructure because each layer is atomically flat, showing long-range correlation on both the c- and a-axis directions, and no interdiffusion at the layer interface. There have been many reports on sample preparation of magnetic GBIC's. As far as we know, however, there have been only a few studies on the magnetic properties of magnetic GBIC's partly because it is difficult to synthesize GBIC's having well-defined c-axis stacking sequences. Suzuki, Oguro, and Jinzaki[13] have studied the magnetic phase transition of $CoCl_2$-$FeCl_3$ GBIC by means of ac magnetic susceptibility in the presence of an external magnetic field perpendicular to the c axis. Rancourt, Hun, and Flandrois[14,15] have studied the magnetic properties of $NiCl_2$-$FeCl_3$ GBIC by using dc magnetic susceptibility in the presence of an external field. Rosenman *et al.*[16] studied the magnetic phase transition of $CoCl_2$-$GaCl_3$ GBIC by using ac magnetic susceptibility. Chehab *et al.*[17,18] have studied the electron-spin resonance (ESR) of $CrCl_3$-$CdCl_2$ GBIC and $CrCl_3$-$MnCl_2$ GBIC. The angular dependence of the ESR linewidth indicates that the 2D spin diffusion occurs in the paramagnetic phase.

In the present work we have synthesized samples of $Co_cNi_{1-c}Cl_2$-$FeCl_3$ GBIC's where the $Co_cNi_{1-c}Cl_2$ layer and $FeCl_3$ layer alternate with a single graphite layer. The separation distance between adjacent $Co_cNi_{1-c}Cl_2$ layers is almost the same as a sum of the c-axis repeat distances for stage-1 $Co_cNi_{1-c}Cl_2$ GIC's and stage-1 $FeCl_3$ GIC. The intraplanar exchange interactions in $Co_cNi_{1-c}Cl_2$ layers and $FeCl_3$ layers are ferromagnetic

and antiferromagnetic, respectively, which may give rise to the coexistence of a ferromagnetic long-range order in $Co_cNi_{1-c}Cl_2$ layers and antiferromagnetic long-range order in the $FeCl_3$ layers at low temperatures. Due to the intervening $FeCl_3$ layer the interplanar interaction between adjacent $Co_cNi_{1-c}Cl_2$ layers in $Co_cNi_{1-c}Cl_2$-$FeCl_3$ GBIC's is expected to be stronger than those in stage-2 $Co_cNi_{1-c}Cl_2$ GIC's. Thus the critical behavior of $Co_cNi_{1-c}Cl_2$-$FeCl_3$ GBIC's is expected to be 3D like, while the critical behavior of stage-2 $Co_cNi_{1-c}Cl_2$ GIC's is 2D like. In $Co_cNi_{1-c}Cl_2$-$FeCl_3$ GBIC's one can also expect the spin-frustration effect arising from the competition between the ferromagnetic intraplanar interaction in the $Co_cNi_{1-c}Cl_2$ layer, the antiferromagnetic intraplanar interaction in the $FeCl_3$ layer, and the interplanar interaction between $Co_cNi_{1-c}Cl_2$ and $FeCl_3$ layers. Furthermore, these interactions depend on the concentration c. Thus the nature of magnetic phase transitions in $Co_cNi_{1-c}Cl_2$-$FeCl_3$ GBIC's is considered to be complicated by the spin-frustration effect and to be dependent on the concentration c.

In this paper we have undertaken an extensive study on the structural and magnetic properties of $Co_cNi_{1-c}Cl_2$-$FeCl_3$ GBIC's over the entire concentration c by using x-ray diffraction, ac and dc magnetic susceptibility, and low- and high-field superconductivity quantum interference device (SQUID) magnetization measurements. The magnetic properties of $Co_cNi_{1-c}Cl_2$-$FeCl_3$ GBIC's are compared with those of stage-2 $Co_cNi_{1-c}Cl_2$ GIC's. We show that a cluster glass phase occurs below T_c in the $Co_cNi_{1-c}Cl_2$ layers of $Co_cNi_{1-c}Cl_2$-$FeCl_3$ GBIC's. We examine the possibility of antiferromagnetic spin order below $T_N(\approx 4$ K) in the $FeCl_3$ layers. We discuss the effect of the interplanar interaction between the $Co_cNi_{1-c}Cl_2$ and $FeCl_3$ layers on the magnetization of $Co_cNi_{1-c}Cl_2$-$FeCl_3$ GBIC's.

II. BACKGROUND

A. Stage-2 $Co_cNi_{1-c}Cl_2$ GIC's

Here we summarize the structural and magnetic properties of stage-2 $Co_cNi_{1-c}Cl_2$ GIC's. These compounds approximate a 2D Heisenberg ferromagnet with XY spin anisotropy,[4,6] where fictitious spin $S=\frac{1}{2}$ for Co^{2+} and $S=1$ for Ni^{2+}. The Co^{2+} and Ni^{2+} spins are randomly distributed on the triangular lattice sites in the $Co_cNi_{1-c}Cl_2$ intercalate layers. The Curie-Weiss temperature Θ monotonically decreases with increasing the Co concentration: $\Theta=70.0$ K at $c=0$ and $\Theta=23.2$ K at $c=1$. The intraplanar exchange interaction between Co^{2+} and Ni^{2+} spins is ferromagnetic and is given by $J(\text{Co-Ni})=\alpha[J(\text{Co-Co})\ J(\text{Ni-Ni})]^{1/2}(=9.88$ K) with $\alpha=1.2$, which is larger than that between like spins: $J(\text{Co-Co})=7.75$ K and $J(\text{Ni-Ni})=8.75$ K. The effective magnetic moments of Co^{2+} and Ni^{2+} spins are given by $P_{\text{eff}}(\text{Co})=5.54\mu_B$ and $P_{\text{eff}}(\text{Ni})=3.29\mu_B$, respectively. The critical temperature T_c monotonically decreases with increasing Co concentration: $T_c=18.38$ K at $c=0$ and $T_c=8.20$ K at $c=1$.[6] The phase transition at T_c is caused by both the XY spin anisotropy effect and the 3D effect through the interplanar exchange interaction. While the interplanar exchange interaction is almost independent of Co concentration, the spin symmetry drastically changes from Heisenberg-like to XY-like with increasing Co concentration. The ratio of T_c to Θ is well described by $T_c/\Theta=Ag_{\text{eff}}^{1/\phi}+B$ with $\phi=1.34$, $A=0.229$ and $B=0.224$, where ϕ is the crossover exponent and the effective XY spin anisotropy g_{eff} gradually increases with the Co concentration: $g_{\text{eff}}=7.62\times10^{-3}$ at $c=0$ and $g_{\text{eff}}=0.48$ at $c=1$.[6] The first and second terms of T_c/Θ are due to the XY spin anisotropy effect in the 2D system and the 3D effect, respectively.

B. Stage-1 and stage-2 $FeCl_3$ GIC's

Here we summarize the structural and magnetic properties of $FeCl_3$ GIC's. In stage-1 and stage-2 $FeCl_3$ GIC's the in-plane structure of the $FeCl_3$ layer forms a honeycomb lattice, where there are two Fe atoms per unit cell with a lattice constant $a_{\text{Fe}}=6.13$ Å. The $FeCl_3$ layer is incommensurate with the graphite layer, where the primitive lattice vector of the $FeCl_3$ layer is rotated by 30° with respect to that of the graphite layer. Ohhashi and Tsujikawa[19] have reported that the dc magnetic susceptibility of $FeCl_3$ GIC for the field directions along a axis and c axis obeys a Curie-Weiss law: $\Theta_a=-8.2\pm0.8$ K, $\Theta_c=-11.4\pm1.8$ K, $P_{\text{eff}}^a=5.98\pm0.05\mu_B$, $P_{\text{eff}}^c=5.87\pm0.07\mu_B$ for stage-1 $FeCl_3$ GIC, and $\Theta_a=-6.0\pm1.0$ K, $\Theta_c=-9.0\pm2.0$ K, $P_{\text{eff}}^a=5.97\pm0.07\mu_B$, $P_{\text{eff}}^c=5.87\pm0.07\mu_B$ for stage-2 $FeCl_3$ GIC, where the a axis corresponds to any direction perpendicular to the c axis. They have also shown that the antiferromagnetic phase transition occurs at $T_N=3.9\pm0.3$ K for stage-1 $FeCl_3$ GIC, and at $T_N=3.6\pm0.3$ K for stage-2 $FeCl_3$ GIC.

Simon and co-workers[20,21] have reported the magnetic neutron-scattering results on powdered samples of stage-1 and stage-2 $FeCl_3$ GIC's, where the c-axis repeat distance is $d=9.45$ Å for stage-1 $FeCl_3$ GIC and $d=12.9$ Å for stage-2 $FeCl_3$ GIC. Below 30 K the magnetic Bragg peak with a Warren shape is observed at the in-plane wavenumber $|\mathbf{Q}_\perp|=0.394\ |\mathbf{a}^+|$ for both stages, where $\mathbf{a}^+$ is the in-plane reciprocal-lattice vector of $FeCl_3$ layers, and is given by $|\mathbf{a}^+|=4\pi/(\sqrt{3}a_{\text{Fe}})=1.185$ Å^{-1}. This result indicates that (i) the in-plane spin structure of Fe^{3+} is incommensurate with the in-plane lattice structure of the $FeCl_3$ layer, and that (ii) a 2D spin correlation develops below 30 K. The integrated intensity of the magnetic Bragg peak at $|\mathbf{Q}_\perp|=0.394\ |\mathbf{a}^+|$ monotonically increases with decreasing temperature from 30 to 1.5 K for both stages. The abrupt increase of the integrated intensity below 3.8 K observed only in the stage-1 $FeCl_3$ GIC indicates that the antiferromagnetic phase transition occurs at $T_N=3.8$ K for the stage-1 $FeCl_3$ GIC. No long-range spin order is observed for stage-2 $FeCl_3$ GIC. Simon *et al.*[21] have also observed a sharp peak at $T_N=3.8$ K in the heat capacity for stage-1 $FeCl_3$ GIC, which is consistent with the results from their neutron-scattering studies.

The spin Hamiltonian for Fe^{3+} ions with spin

$S(=5/2)$ in $FeCl_3$ GIC is described by[19]

$$H=-2J(\text{Fe-Fe})\sum_{\langle i,j\rangle}\mathbf{S}_i\cdot\mathbf{S}_j+D(\text{Fe})\sum_i(S_i^z)^2\,, \qquad (1)$$

where J(Fe-Fe) is the intraplanar exchange interaction and is given by -0.47 K for stage-1 $FeCl_3$ GIC and by -0.34 K for stage-2 $FeCl_3$ GIC, respectively, and D(Fe) is the single ion anisotropy and is given by 0.13 K for stage-1 $FeCl_3$ GIC and 0.23 K for stage-2 $FeCl_3$ GIC. Thus the $FeCl_3$ GIC's magnetically behave like an XY-like antiferromagnet.[19]

III. EXPERIMENTAL PROCEDURE

Samples of $Co_cNi_{1-c}Cl_2$-$FeCl_3$ GBIC's were prepared by a sequential intercalation method:[13] the intercalant $FeCl_3$ was intercalated into the empty graphite galleries of stage-2 $Co_cNi_{1-c}Cl_2$ GIC. A mixture of well-defined stage-2 $Co_cNi_{1-c}Cl_2$ GIC based on single-crystal kish graphite and single-crystal $FeCl_3$ was sealed in vacuum inside Pyrex glass tubing, and was kept at 330 °C for two weeks. The $(00L)$ x-ray diffraction at 300 K was measured by using a Huber double-circle diffractometer with a Siemens 2.0 kW x-ray generator. The $Co_cNi_{1-c}Cl_2$-$FeCl_3$ GBIC samples were confirmed to have well-defined c-axis stacking sequences of -G-$Co_cNi_{1-c}Cl_2$-G-FeCl-G-$Co_cN_{1-c}Cl_2$-G-$FeCl_3$-G- .

The dc magnetic susceptibility of $Co_cNi_{1-c}Cl_2$-$FeCl_3$ GBIC samples was measured by a Faraday balance method in the temperature range between 1.5 and 300 K. The magnetic field of 100 Oe $\le H \le$ 2 kOe was applied to any direction perpendicular to the c axis. The ac magnetic susceptibility of the GBIC samples was measured by an ac Hartshorn bridge method in the temperature range between 4.2 and 25 K. An ac magnetic field with frequency $\nu=330$ Hz and amplitude $h=300$ m Oe was applied along any direction perpendicular to the c axis. The SQUID magnetization measurements were carried out with a SQUID magnetometer (Model VTS-905 SQUID system, S.H.E. Corporation). The low-field SQUID magnetization measurements were performed in the following steps: (i) A sample having a weight of 4–7 mg was first cooled to a temperature T_1 from 300 K in five min in the absence of external magnetic field: $T_1=2$ K for $CoCl_2$-$FeCl_3$ GBIC, and $T_1=4.2$ K for $Co_cNi_{1-c}Cl_2$-$FeCl_3$ GBIC's with $c=0$, 0.25, and 0.75. A field of 1 Oe was then applied along any direction perpendicular to the c axis. (ii) The temperature dependence of zero-field-cooled (ZFC) magnetization, M_{ZFC}, was measured while increasing temperature from T_1 to T_2:$T_2=10$ K for $CoCl_2$-$FeCl_3$ GBIC, and $T_2=30$ K for $Co_cNi_{1-c}Cl_2$-$FeCl_3$ GBIC's with $c=0$, 0.25, and 0.75. (iii) The sample was again cooled in the field of 1 Oe and the temperature dependence of field-cooled (FC) magnetization, M_{FC}, was measured while decreasing temperature from T_2 to T_1.

IV. RESULT

A. Stoichiometry and structure

The stoichiometry of GBIC samples used in the present work, $C_n(Co_cNi_{1-c}Cl_2)_{1-b}(FeCl_3)_b$, was determined from three consecutive weight uptake measurements on (i) pristine graphite before intercalation, (ii) stage-2 $Co_cNi_{1-c}Cl_2$ GIC after the intercalation of $Co_cNi_{1-c}Cl_2$ into the pristine graphite, and (iii) $Co_cNi_{1-c}Cl_2$-$FeCl_3$ GBIC after the sequential intercalation of $FeCl_3$ into stage-2 $Co_cNi_{1-c}Cl_2$ GIC. The concentrations of C and Fe for the $Co_cNi_{1-c}Cl_2$-$FeCl_3$ GBIC samples thus determined are listed in Table I as n and b, respectively. The concentration b is found to be between 0.3 and 0.4 except for the samples with $c=0.5$ and 0.55. Here we compare the stoichiometry of $Co_cNi_{1-c}Cl_2$-$FeCl_3$ GBIC samples with the ideal one of MCl_2-$FeCl_3$ GBIC (M = Co, Ni) which is derived as follows. The in-plane structure of the MCl_2 layer in MCl_2-$FeCl_3$ GBIC is assumed to be the same as that of stage-2 MCl_2 GIC. The MCl_2 layer forms a triangular lattice with the lattice constants $a_M=3.46$ Å for Ni and 3.55 Å for Co.[22] In the MCl_2 layer there is one M atom per unit cell of area $\sqrt{3}a_M^2/2$. On the other hand, the graphite layer and $FeCl_3$ layer are assumed to form honeycomb lattices with lattice constants $a_G=2.46$ Å and $a_{Fe}=6.13$ Å,[19] respectively. In the $FeCl_3$ layer, for example, there are two Fe atoms per unit cell of area $\sqrt{3}a_{Fe}^2/2$. Thus the ideal stoichiometry of MCl_2-$FeCl_3$ GBIC is calculated as $C_n(MCl_2)_{1-b}(FeCl_3)_b$ with $b=2/[(a_{Fe}^2/a_M^2)+2]$ and $n=2b(a_{Fe}^2/a_G^2)$:$n=4.83$ and $b=0.39$ for Ni, and $n=4.99$, $b=0.40$ for Co. One can expect that the ideal value of b for $Co_cNi_{1-c}Cl_2$-$FeCl_3$ GBIC's is between 0.39 and 0.40. The concentration b of $Co_cNi_{1-c}Cl_2$-$FeCl_3$ GBIC samples is found to be close to this ideal value of b, which suggests that the $FeCl_3$ layer forms a honeycomb lattice with the same lattice constant a_{Fe} as stage-1 and stage-2 $FeCl_3$ GIC's.

The $(00L)$ x-ray-diffraction patterns of stage-2 $Co_cNi_{1-c}Cl_2$ GIC samples used as starting compounds and $Co_cNi_{1-c}Cl_2$-$FeCl_3$ GBIC's have been taken at 300 K. For the stage-2 $Co_cNi_{1-c}Cl_2$ GIC's sharp Bragg peaks are observed at the wave number $Q_c=(2\pi/d)L$ where d is the c-axis repeat distance and is almost independent of Co concentration ($d=12.70\pm0.04$ Å).[5] As $FeCl_3$ intercalants are sequentially intercalated into the empty graphite galleries of the stage-2 $Co_cNi_{1-c}Cl_2$ GIC's, the c-axis repeat distance d is expected to change drastically. Figure 1(a) shows a typical example of $(00L)$

TABLE I. Stoichiometry of $Co_cNi_{1-c}Cl_2$-$FeCl_3$ GBIC samples $C_n(Co_cNi_{1-c}Cl_2)_{1-b}$ $(FeCl_3)_b$ and c-axis repeat distance d (Å), where b is the Fe concentration determined from weight-uptake measurements.

Sample No.	c	n	b	d (Å)
1	0	6.46	0.30	18.80±0.25
2	0.05	12.5	0.31	
3	0.25	9.88	0.39	18.73±0.21
4	0.4	10.0	0.34	18.51±0.52
5	0.5	8.93	0.28	18.76±0.38
6	0.55	11.6	0.20	18.88±0.18
7	0.75	7.74	0.40	18.90±0.06
8	0.9	7.94	0.32	18.74±0.48
9	1	6.40	0.37	18.77±0.46

x-ray-diffraction pattern for $Co_cNi_{1-c}Cl_2$-$FeCl_3$ GBIC's with $c=0.75$. The Bragg reflections indexed to GBIC $(00L)$ are observed at the wave number $Q_c=(2\pi/d)L$ where the c-axis repeat distance $d(=18.90\pm0.06$ Å) coincides with a sum of those of stage-1 $CoCl_2$ GIC ($d_{Co}=9.38$ Å) (Ref. 22) and stage-1 $FeCl_3$ GIC ($d_{Fe}=9.45$ Å).[21] The Bragg reflection indexed to stage-2 (002) observed around $Q_c=1$ Å^{-1} indicates that this GBIC sample has small fractions of stage-2 GIC in which $FeCl_3$ bulk intercalants are not intercalated on sequential intercalation. The GBIC $(00L)$ reflections with odd integer L cannot be observed because of the following reasons: (i) the structure factor of the $FeCl_3$ layer is similar to that of the $Co_cNi_{1-c}Cl_2$ layer and (ii) the distance of the package G-$FeCl_3$-G along the c axis is almost the same as that of the package G-$Co_cNi_{1-c}Cl_2$-G along the c axis. The mosaic spread of GBIC's is typically about 10°–16° and is much larger than that of stage-2 GIC (about 5°–7°).

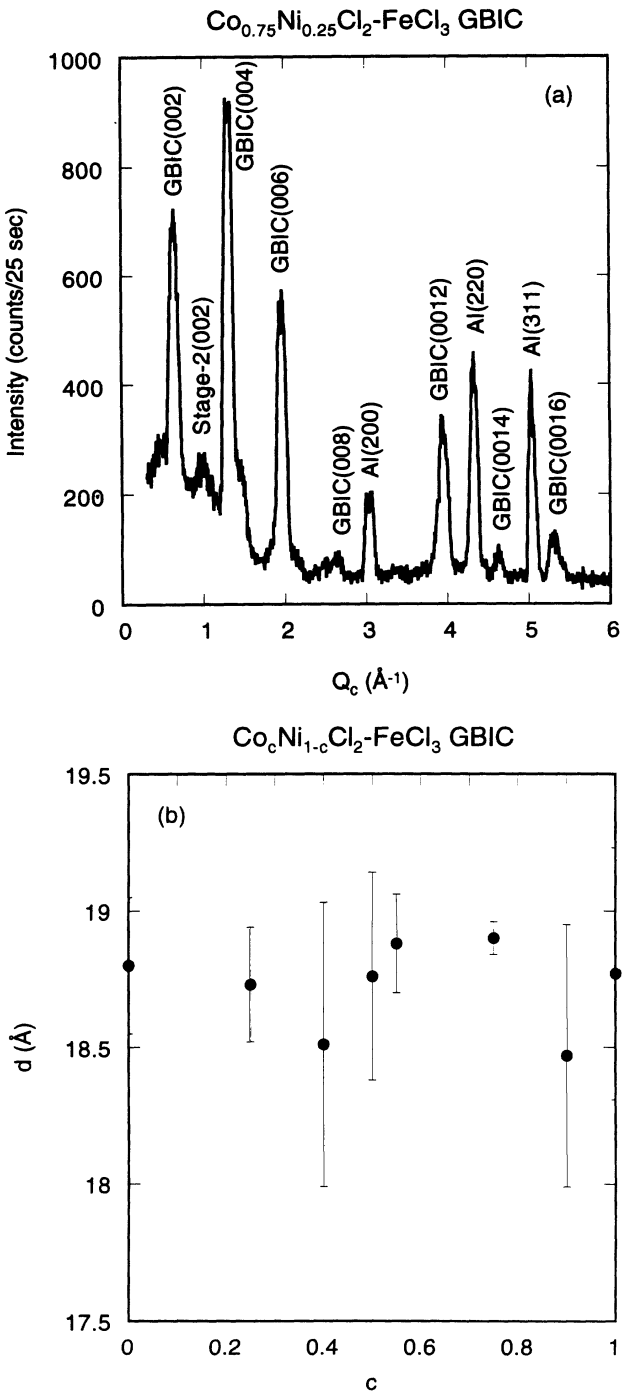

FIG. 1. (a) $(00L)$ x-ray-diffraction pattern for $Co_cNi_{1-c}Cl_2$-$FeCl_3$ GBIC's with $c=0.75$ at room temperature. Peaks are indexed to stage-2 GIC and GBIC. There is a contribution from the Al sample holder. (b) c-axis repeat distance d vs concentration c for $Co_cNi_{1-c}Cl_2$-$FeCl_3$ GBIC's.

The c-axis repeat distance d of $Co_cNi_{1-c}Cl_2$-$FeCl_3$ GBIC samples used in the present work is determined from their $(00L)$ x-ray diffraction and is listed in Table I. Figure 1(b) shows the plot of d vs concentration c for $Co_cNi_{1-c}Cl_2$-$FeCl_3$ GBIC's. In spite of the observed large uncertainty in d which is due to the c-axis stacking disorder of GBIC's, the c-axis repeat distance seems to be independent of the concentration c: $d=18.69\pm0.22$ Å^{-1}.

B. Paramagnetic susceptibility

For the study of the magnetic properties of $Co_cNi_{1-c}Cl_2$-$FeCl_3$ GBIC's, the dc magnetic susceptibility of $Co_cNi_{1-c}Cl_2$-$FeCl_3$ GBIC's with $c=0$, 0.05, 0.25, 0.4, 0.5, 0.55, 0.75, 0.9, and 1 was measured at $H=2$ kOe in the temperature range between 20 and 300 K. The magnetic field was applied along any direction perpendicular to the c axis. A least-squares fit of the dc magnetic-susceptibility data for $150\leq T\leq 300$ K to the Curie-Weiss law

$$\chi_M=\frac{C_M}{T-\Theta}+\chi_M^0 , \tag{2}$$

yields values of the Curie-Weiss constant C_M (emu K/av mol), the Curie-Weiss temperature Θ (K), and the temperature-independent susceptibility χ_M^0 (emu/av mol). The values of C_M, Θ, and χ_M^0 for $Co_cNi_{1-c}Cl_2$-$FeCl_3$ GBIC's are listed in Table II. Figure 2 shows the reciprocal susceptibility $(\chi_M-\chi_M^0)^{-1}$ as a function of temperature for $Co_cNi_{1-c}Cl_2$-$FeCl_3$ GBIC's

TABLE II. Θ (K), C_M (emu K/av mol), $P_{\text{eff}}(\mu_B/\text{av atom})$, χ_M^0 (10^{-3} emu/av mol) for $Co_cNi_{1-c}Cl_2$-$FeCl_3$ GBIC's.

Sample No.	c	Θ	C_M	P_{eff}	χ_M^0
1	0	4.47±0.58	2.04	4.04	0.26±0.08
2	0.05	47.89±0.30	2.43	4.41	−0.18±0.02
3	0.25	34.16±0.26	2.94	4.85	−0.36±0.02
4	0.4	31.52±0.38	3.48	5.28	−0.46±0.03
5	0.5	25.02±0.19	4.00	5.66	−0.80±0.02
6	0.55	29.47±0.29	3.75	5.47	−0.70±0.02
7	0.75	23.80±0.52	3.90	5.59	−0.35±0.04
8	0.9	23.16±0.16	3.95	5.62	−0.88±0.01
9	1	21.99±0.15	3.78	5.50	−0.03±0.01

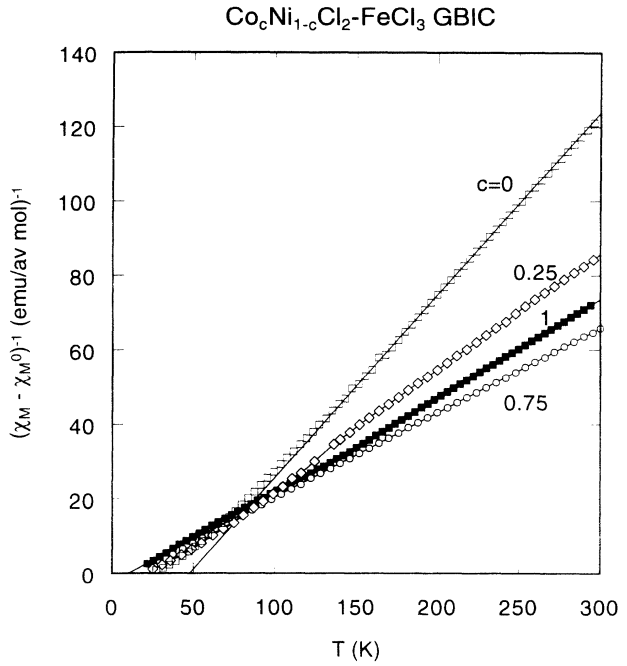

FIG. 2. Reciprocal susceptibility $(\chi_M - \chi_M^0)^{-1}$ vs T for $Co_cNi_{1-c}Cl_2$-$FeCl_3$ GBIC's with $c=0$ (□), 0.25 (◇), 0.75 (○), and 1 (■), where χ_M^0 is a temperature-independent susceptibility listed in Table II. The solid lines denote the Curie-Weiss law described by Eq. (2) with C_M, Θ, and χ_M^0 listed in Table II.

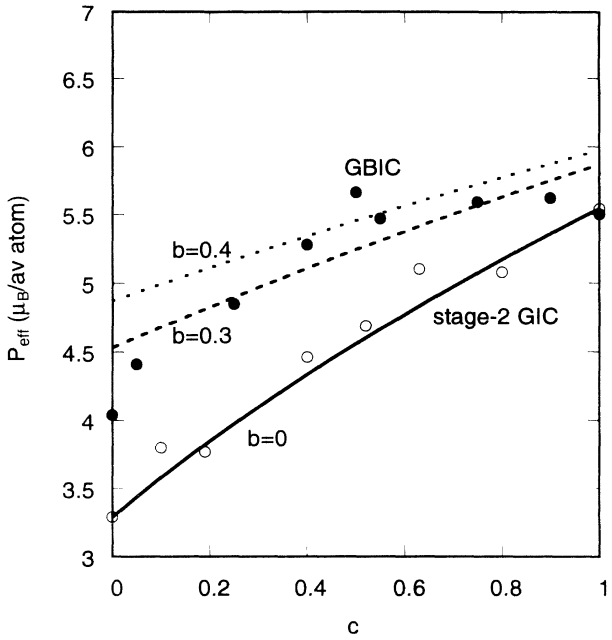

FIG. 3. Effective magnetic moment P_{eff} as a function of concentration c for $Co_cNi_{1-c}Cl_2$-$FeCl_3$ GBIC's (●) and stage-2 $Co_cNi_{1-c}Cl_2$ GIC's (○). The solid line, dashed line, and dotted line are described by Eq. (5) with $b=0$, 0.3, and 0.4, respectively, where $P_{eff}=6.57\mu_B$ for stage-2 $FeCl_3$ GIC.

with $c=0$, 0.25, 0.75, and 1. The dc magnetic susceptibility is found to obey the Curie-Weiss law above 150 K.

Figure 3 shows the effective magnetic moment P_{eff} vs concentration c for $Co_cNi_{1-c}Cl_2$-$FeCl_3$ GBIC's (closed circles), where P_{eff} is related to C_M by $C_M = N_A\mu_B^2 P_{eff}^2/3k_B \approx P_{eff}^2/8$ and N_A is the Avogadro's number. For comparison the plot of P_{eff} vs c for stage-2 $Co_cNi_{1-c}Cl_2$ GIC's (open circles) is also shown in Fig. 3. The value of P_{eff} for $Co_cNi_{1-c}Cl_2$-$FeCl_3$ GBIC's is larger than that for stage-2 $Co_cNi_{1-c}Cl_2$ GIC's for the same concentration c. Figure 4 shows the Curie-Weiss temperature Θ vs concentration c for $Co_cNi_{1-c}Cl_2$-$FeCl_3$ GBIC's denoted by closed circles, where Θ is equal to $2zJS(S+1)/3$ for the system with the nearest-neighbor interaction of $-2J\mathbf{S}_i\cdot\mathbf{S}_j$, and z is the number of nearest-neighbor spins. For comparison the data of Θ vs c for stage-2 $Co_cNi_{1-c}Cl_2$ GIC's denoted by open circles are also shown in Fig. 4. The positive sign for Θ in $Co_cNi_{1-c}Cl_2$-$FeCl_3$ GBIC's and stage-2 $Co_cNi_{1-c}Cl_2$ GIC's for any concentration c indicates that the average intraplanar exchange interaction is ferromagnetic. The value of Θ for $Co_cNi_{1-c}Cl_2$-$FeCl_3$ GBIC's is smaller than that for stage-2 $Co_cNi_{1-c}Cl_2$ GIC's for any concentration c. This drastic decrease of Θ is due to the antiferromagnetic intraplanar exchange interaction between Fe^{3+} spins in the $FeCl_3$ layers. The magnetic behavior of the $FeCl_3$ layer in $Co_cNi_{1-c}Cl_2$-$FeCl_3$ GBIC's is considered

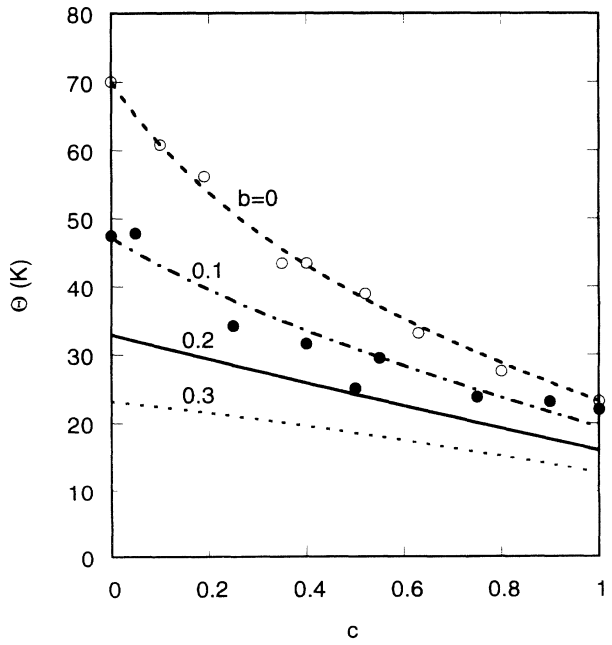

FIG. 4. Curie-Weiss temperature Θ as a function of concentration c for $Co_cNi_{1-c}Cl_2$-$FeCl_3$ GBIC's (●) and stage-2 $Co_cNi_{1-c}Cl_2$ GIC's (○). The dashed line, dash dotted line, solid line, and dotted line are described by Eq. (7) with $b=0$, 0.1, 0.2, and 0.3, respectively.

to be essentially the same as that in stage-2 $FeCl_3$ GIC. In the present work we have measured the temperature dependence of dc magnetic susceptibility for stage-2 $FeCl_3$ GIC. The Curie-Weiss temperature and the effective magnetic moment are determined as $\Theta = -4.3 \pm 0.2$ K and $P_{\text{eff}} = 6.57 \mu_B$. This Curie-Weiss temperature is close to the values reported by Ohhashi and Tsujikawa[19] ($\Theta^a = -6.0 \pm 1.0$ K). The negative sign of Θ indicates that the intraplanar exchange interaction between Fe^{3+} spins is antiferromagnetic. The effective magnetic moment is different from the value reported by Ohhashi and Tsujikawa[19] ($P_{\text{eff}} = 5.97 \mu_B$).

In Sec. V A, the concentration dependence of P_{eff} and Θ for $Co_cNi_{1-c}Cl_2$-$FeCl_3$ GBIC's and stage-2 $Co_cNi_{1-c}Cl_2$ GIC's will be discussed in comparison with the predictions from the molecular field theory, which are shown by the several lines in Figs. 3 and 4.

C. Magnetic phase transition

We have studied the magnetic phase transition of $Co_cNi_{1-c}Cl_2$-$FeCl_3$ GBIC's from dc and ac magnetic susceptibility at low temperatures. Figure 5(a) shows the temperature dependence of dc magnetic susceptibility for $Co_cNi_{1-c}Cl_2$-$FeCl_3$ GBIC's with $c = 0$, 0.25, 0.4, 0.5, 0.75, 0.9, and 1 in the temperature range between 1.5 and 25 K. The magnetic field ($H = 100$ Oe) was applied along any direction perpendicular to the c axis. The dc magnetic susceptibility at low temperatures corresponds to the ratio M/H where M is the magnetization. For comparison, in Fig. 5(b) we show the temperature dependence of dc magnetic susceptibility for stage-2 $Co_cNi_{1-c}Cl_2$ GIC's with $c = 0$, 0.1, 0.19, 0.4, 0.52, 0.8, and 1. We find from Fig. 5(a) that the magnetization M of $Co_cNi_{1-c}Cl_2$-$FeCl_3$ GBIC's ($0 \le c \le 1$) drastically decreases with increasing temperature and shows a tail around a critical temperature T_c, which prevents determining an exact value of T_c. In order to estimate the value of T_c, here we assume that the temperature dependence of M near T_c is described by the smeared power law with a critical exponent β[5]

$$M(T) = M(0) \int_T^{\infty} A \left[1 - \frac{T}{T_c} \right]^{\beta} f(T_c) dT_c \ , \tag{3}$$

where A is a constant, $M(T)$ is the magnetization at the temperature T, and $f(T_c)$ is a Gaussian distribution of T_c which is given by

$$f(T_c) = \frac{1}{\sqrt{2\pi}\sigma} \exp \left[-\frac{1}{2} \left[\frac{T_c - \langle T_c \rangle}{\sigma} \right]^2 \right] , \tag{4}$$

with the average value $\langle T_c \rangle$ and the width σ. The values of β, $\langle T_c \rangle$, and σ are determined from the least-squares fit and are listed in Table III. The width σ is a measure for the smearing of T_c: $1.02 \le \sigma \le 2.10$ K. These values of σ are on the same order as those of stage-2 $Co_cNi_{1-c}Cl_2$ GIC's:[5] ($0.62 \le \sigma \le 2.24$ K). The critical temperature $\langle T_c \rangle$ monotonically decreases with increasing the concentration c: $\langle T_c \rangle = 21.75 \pm 0.05$ K at $c = 0$ and 9.23 ± 0.05 K at $c = 1$. This concentration dependence of $\langle T_c \rangle$ for $Co_cNi_{1-c}Cl_2$-$FeCl_3$ GBIC's is very similar to that for stage-2 $Co_cNi_{1-c}Cl_2$ GIC's,[5] suggesting that GBIC's with any concentration c undergo a ferromagnetic phase transition associated with the in-plane ferromagnetic spin ordering inside the $Co_cNi_{1-c}Cl_2$ layers. Figure 6(a) shows the plot of the exponent β vs concentration c for $Co_cNi_{1-c}Cl_2$-$FeCl_3$

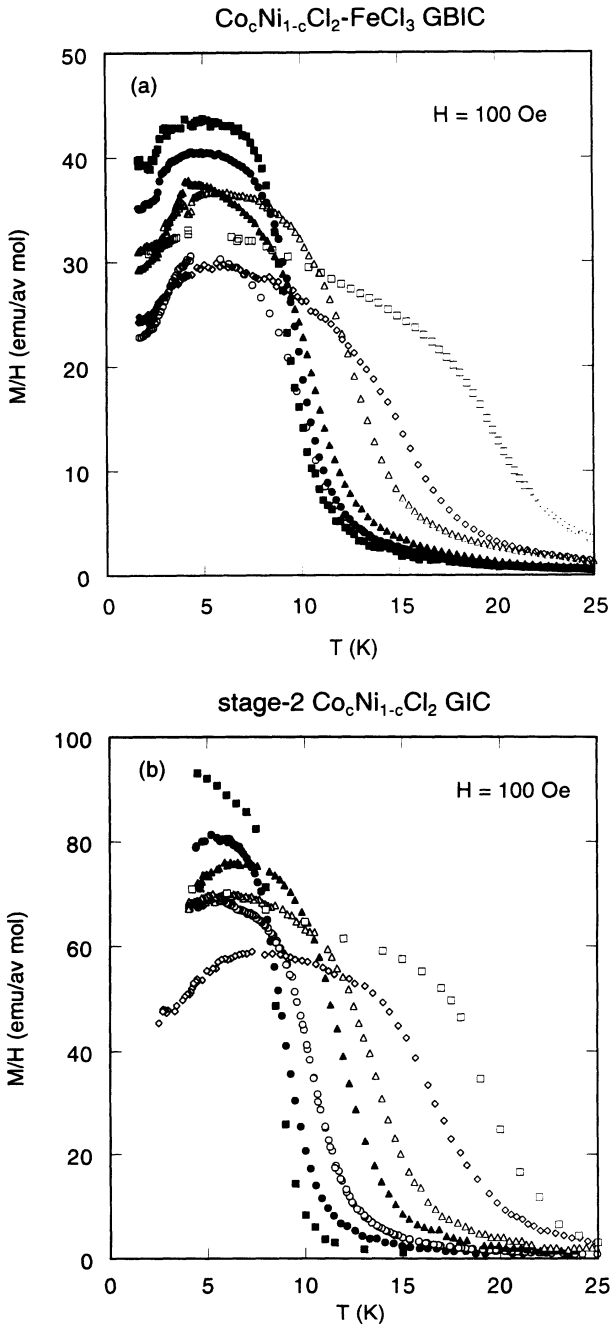

FIG. 5. (a) Temperature dependence of dc magnetic susceptibility for $Co_cNi_{1-c}Cl_2$-$FeCl_3$ GBIC's with $c = 0$ (□), 0.25 (◇), 0.4 (△), 0.5 (▲), 0.75 (○), 0.9 (●), and 1 (■), where $H = 100$ Oe and H⊥c. (b) Temperature dependence of dc magnetic susceptibility for stage-2 $Co_cNi_{1-c}Cl_2$ GIC's with $c = 0$ (□), 0.1 (◇), 0.19 (△), 0.4 (▲), 0.52 (○), 0.8 (●), and 1 (■), where $H = 100$ Oe and H⊥c (Ref. 5).

TABLE III. Average critical temperature $\langle T_c \rangle$ (K), and critical temperature T_c (K), critical exponent β, and width σ (K) for $Co_cNi_{1-c}Cl_2$-$FeCl_3$ GBIC's.

Sample No.	c	$\langle T_c \rangle$	T_c	β	σ
1	0	21.75	19.48	0.37	1.75
2	0.05	20.51	15.66	0.36	1.69
3	0.25	17.07	13.92	0.39	2.10
4	0.4	13.89	11.82	0.27	1.58
5	0.5	11.54	9.58	0.30	1.09
6	0.55	12.52	10.38	0.27	1.16
7	0.75	11.32	9.16		
8	0.9	10.34	8.96	0.14	1.04
9	1	9.23	9.10	0.03	1.02

GBIC's and stage-2 $Co_cNi_{1-c}Cl_2$ GIC's.[5] The value of β for stage-2 GIC's is almost independent of concentration c: $\beta \approx 0.1$. On the other hand, the value of β for GBIC's decreases from $\beta = 0.37 \pm 0.02$ at $c = 0$ to $\beta = 0.03 \pm 0.02$ at $c = 1$. These results imply that the universality class of critical behavior in GBIC's is very different from that in stage-2 GIC's at least in the concentration range $0 \leq c \leq 0.55$. Approximate values of β are given for various spin models as $\beta = 0.367$ for a 3D Heisenberg spin system, 0.345 for a 3D XY spin system, and 0.125 for a 2D Ising system.[23] The large value of β for GBIC's with $0 \leq c \leq 0.55$ indicates that these GBIC's magnetically behave like a 3D Heisenberg spin system with XY spin anisotropy. The interplanar interaction between adjacent $Co_cNi_{1-c}Cl_2$ layers in GBIC's is stronger than that in stage-2 GIC's. The small value of β observed for GBIC's with $c = 0.9$ and 1, which is almost the same as that of stage-2 GIC's, demonstrates that these GBIC's approximate 2D Heisenberg spin systems with XY spin anisotropy. Like stage-2 $Co_cNi_{1-c}Cl_2$ GIC's, the magnetic phase transition of $Co_cNi_{1-c}Cl_2$-$FeCl_3$ GBIC's is considered to be driven mainly by the 2D ferromagnetic spin ordering of the $Co_cNi_{1-c}Cl_2$ layers. The interplanar exchange interaction J' between adjacent $Co_cNi_{1-c}Cl_2$ layers is enhanced by the incorporation of $FeCl_3$. Because of this increase of $|J'|$ the 2D and 3D spin orderings are considered to occur almost simultaneously.

Since the stage-2 $FeCl_3$ GIC undergoes an antiferromagnetic phase transition at $T_N = 3.6 \pm 0.3$ K,[19] the magnetization M of $Co_cNi_{1-c}Cl_2$-$FeCl_3$ GBIC's around T_N is expected to be influenced by a possible antiferromagnetic long-range order in the $FeCl_3$ layers at low temperatures near T_N. In fact we find from Fig. 5(a) that the magnetization M of $Co_cNi_{1-c}Cl_2$-$FeCl_3$ GBIC's with $c = 0.75$, 0.9, and 1 exhibits a pronounced plateaulike peak centered at 5 K, much lower than T_c. As shown in Fig. 5(b) such a plateaulike peak is not clearly observed for stage-2 $Co_cNi_{1-c}Cl_2$ GIC's with the same concentration c, although the data of stage-2 GIC's below 4 K are missing. In GBIC's a ferromagnetic long-range order within $Co_cNi_{1-c}Cl_2$ layers is established below T_c, a temperature which is much higher than 5 K. The plateaulike peak of M at 5 K is considered to be closely related to the growth of short-range spin order occurring in $FeCl_3$ layers. The drastic decrease of M below 4 K is considered to be due to the appearance of antiferromagnetic long-range order of Fe^{3+} spins: $T_N \approx 4$ K. We note that a slight decrease of M with decreasing temperature is observed below 6 K in stage-2 $Co_cNi_{1-c}Cl_2$ GIC's [Fig. 5(b)]. This is due to the antiferromagnetic spin order of $Co_cNi_{1-c}Cl_2$ layers along the c axis through an extremely weak antiferromagnetic interplanar exchange interaction between adjacent $Co_cNi_{1-c}Cl_2$ layers. Figure 6(b) shows

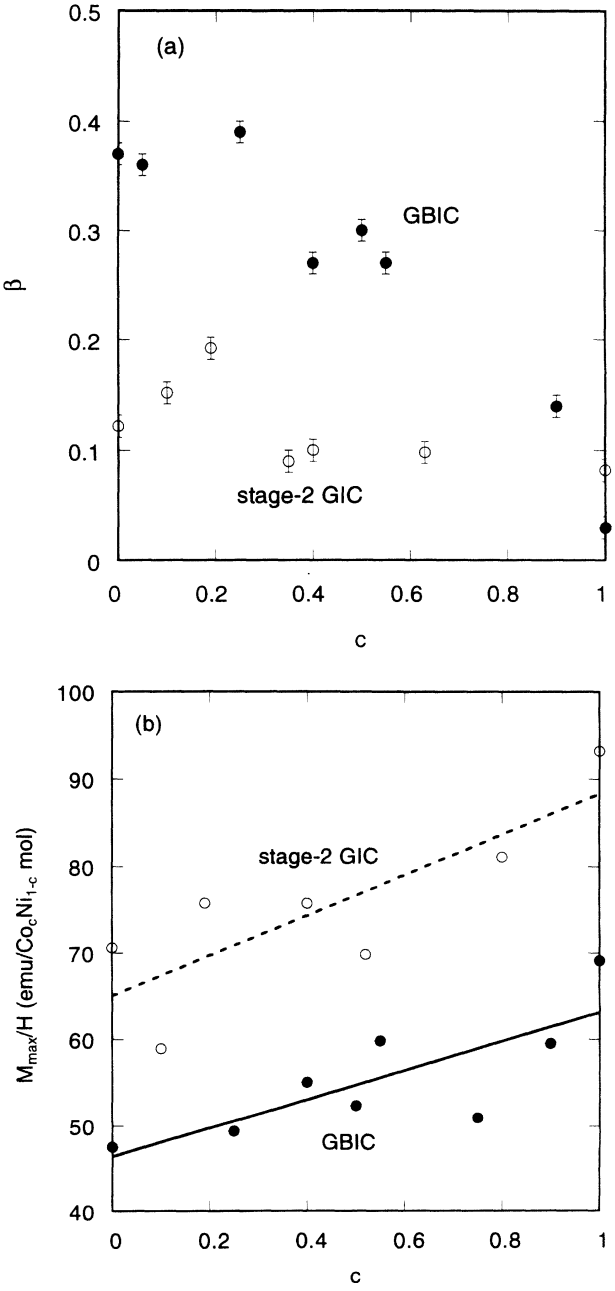

FIG. 6. (a) Critical exponent β vs concentration c for $Co_cNi_{1-c}Cl_2$-$FeCl_3$ GBIC's (●) and stage-2 $Co_cNi_{1-c}Cl_2$ GIC's (○). (b) M_{max}/H (emu/Co_cNi_{1-c} av mol) vs concentration c for $Co_cNi_{1-c}Cl_2$-$FeCl_3$ GBIC's and stage-2 $Co_cNi_{1-c}Cl_2$ GIC's. The solid and dotted lines are guides to the eyes.

the maximum susceptibility defined by $\chi_{max}(=M_{max}/H)$ per Co_cNi_{1-c} mol as a function of temperature for $Co_cNi_{1-c}Cl_2$-$FeCl_3$ GBIC's and stage-2 $Co_cNi_{1-c}Cl_2$ GIC's,[5] where M_{max} is the maximum value of M. We find that for both GBIC's and stage-2 GIC's, χ_{max} tends to increase linearly with the concentration c: $\chi_{max}=46.4+16.7c$ (emu/Co_cNi_{1-c} mol) for GBIC's (solid line) and $\chi_{max}=65.0+23.3c$ (emu/Co_cNi_{1-c} mol) for GIC's (dashed line). For the same concentration c, the value of χ_{max} for stage-2 GIC is approximately 1.4 times as large as that for GBIC's. The Co^{2+} and Ni^{2+} spins are ferromagnetically aligned along the direction of the external magnetic field. On the other hand, the direction of Fe^{3+} spins is antiparallel to these ferromagnetic spins because of the interplanar interaction between $Co_cNi_{1-c}Cl_2$ and $FeCl_3$ layers as will be discussed in Sec. V C. This leads to a drastic decrease of χ_{max} in GBIC's. When the magnetization of one $FeCl_3$ layer and one $Co_cNi_{1-c}Cl_2$ layer along the field direction is assumed to be given by M_{Fe} and $M_{Co\text{-}Ni}$, respectively, M_{Fe} is estimated as $M_{Fe}=-0.29M_{Co\text{-}Ni}$ since $M_{Co\text{-}Ni}/(M_{Co\text{-}Ni}+M_{Fe})=1.4$.

In order to determine a critical temperature T_c more exactly, we have measured the temperature dependence of ac magnetic susceptibility for $Co_cNi_{1-c}Cl_2$-$FeCl_3$ GBIC's with $c=0$, 0.05, 0.25, 0.4, 0.5, 0.55, 0.75, 0.9, and 1 in the temperature range between 4.2 and 25 K. Figure 7(a) shows the typical examples of the real part of ac magnetic susceptibility χ' vs temperature for $Co_cNi_{1-c}Cl_2$-$FeCl_3$ GBIC's with $c=0$, 0.25, 0.4, and 0.75. The real part χ' shows a broad peak at the critical temperature T_c listed in Table III. This peak becomes broader with decreasing concentration c. Figure 7(b) shows the plot of T_c vs concentration c for $Co_cNi_{1-c}Cl_2$-$FeCl_3$ GBIC's (closed circles) and stage-2 $Co_cNi_{1-c}Cl_2$ GIC's (open circles). These data are determined from the ac magnetic susceptibility. The critical temperature of GBIC's is almost the same as that of stage-2 GIC's with the same concentration c: T_c rapidly decreases with increasing the concentration c for $0\le c\le 0.5$, and is almost constant for $0.75\le c\le 1$. The value of T_c for GBIC's with $c=0$ and 1 is slightly larger than that of stage-2 GIC's. These results indicate that the ferromagnetic long-range order occurring in the $Co_cNi_{1-c}Cl_2$ layers is mainly responsible for the magnetic phase transition of $Co_cNi_{1-c}Cl_2$-$FeCl_3$ GBIC's at T_c.

D. SQUID magnetization

In order to study the details of the magnetic phase transition of T_c, we have measured the temperature dependence of low-field SQUID magnetization for $Co_cNi_{1-c}Cl_2$-$FeCl_3$ GBIC's. Figure 8 shows typical examples of the temperature dependence of ZFC magnetization (M_{ZFC}), and FC magnetization (M_{FC}), and difference $\delta(=M_{FC}-M_{ZFC})$ for $Co_cNi_{1-c}Cl_2$-$FeCl_3$ GBIC's with (a) $c=1$, (b) $c=0.75$, (c) $c=0.25$, and (d) $c=0$. For each concentration M_{FC} drastically increases below T_c with decreasing temperature. The saturated value of M_{FC} changes from ≈ 300 emu/av mol at $c=0$ to ≈ 700 emu/av mol at $c=1$ with the concentration c. On the other hand, the magnetization M_{ZFC} deviates downward from M_{FC} below T_c and shows a broad peak at T_{max} which is lower than T_c. The difference δ is a measure of the irreversible effect of magnetization for GBIC's. For $c=1$, 0.25, and 0 the difference δ monoton-

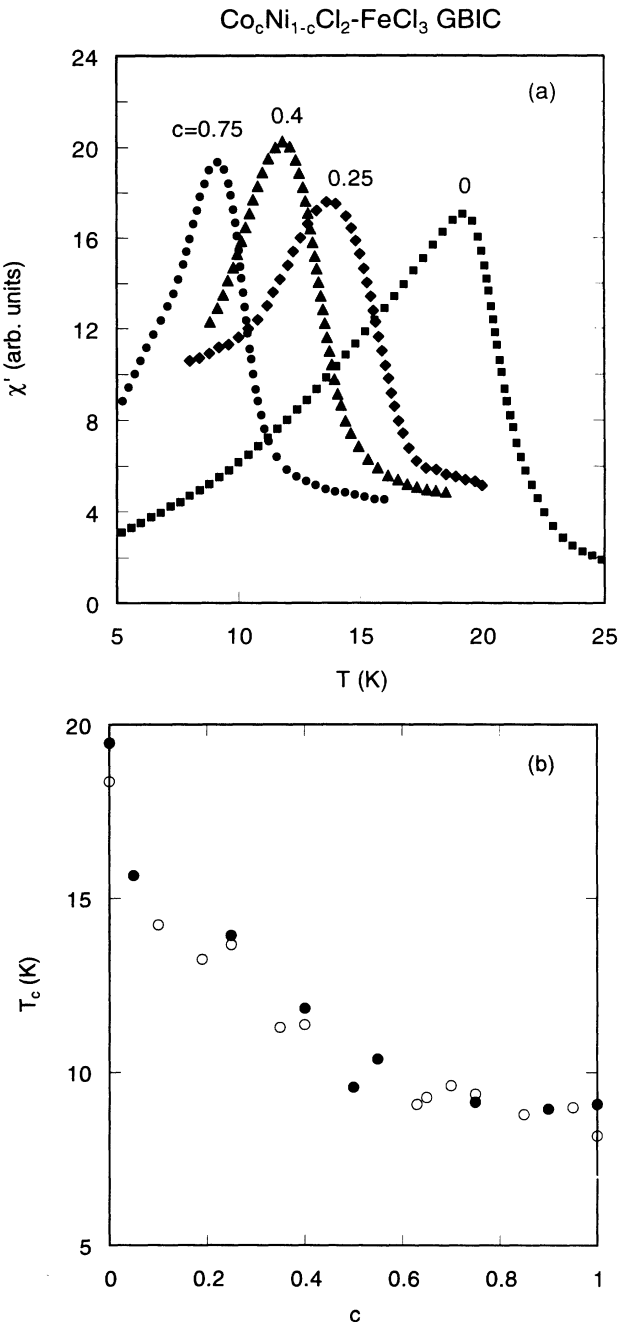

FIG. 7. (a) Temperature dependence of real part of ac magnetic susceptibility χ' of $Co_cNi_{1-c}Cl_2$-$FeCl_3$ GBIC's with $c=0$ (■), 0.25 (◆) 0.4 (▲), and 0.75 (●). The ac magnetic field of $\nu=330$ Hz and $h=300$ m Oe is applied along any direction perpendicular to the c axis. (b) Critical temperature T_c as a function of concentration c for $Co_cNi_{1-c}Cl_2$-$FeCl_3$ GBIC's (●) and stage-2 $Co_cNi_{1-c}Cl_2$ GIC's (○) determined from the ac magnetic-susceptibility measurements.

ically decreases with increasing temperature and reduces to zero at T_c. For $c=0.75$, δ does not reduce to zero even at 25 K, far above $T_c(\approx 10$ K). For any concentration c there is no anomaly in δ around T_{max} suggesting that T_{max} is not a magnetic phase transition point of the systems. Since the temperature dependence of M_{FC}, M_{ZFC}, and δ in $Co_cNi_{1-c}Cl_2$-$FeCl_3$ GBIC's is similar to those in stage-2 $Co_cNi_{1-c}Cl_2$ GIC's,[24] the magnetic phase transition of $Co_cNi_{1-c}Cl_2$-$FeCl_3$ GBIC's at T_c is essentially the same as that of stage-2 $Co_cNi_{1-c}Cl_2$ GIC's. The irreversible effect of magnetization is a phenomenon accompanied with the growth of the in-plane spin order inside the $Co_cNi_{1-c}Cl_2$ layers. In a previous paper[24] it was shown that the magnetic phase transition of stage-2 $Co_cNi_{1-c}Cl_2$ GIC's can be qualitatively explained in terms of a cluster-glass-phase model. We think that the low-temperature phase below T_c in $Co_cNi_{1-c}Cl_2$-$FeCl_3$ GBIC's is also a cluster-glass phase. The details of the cluster-glass phase in $Co_cNi_{1-c}Cl_2$-$FeCl_3$ GBIC's will be discussed in Sec. V.

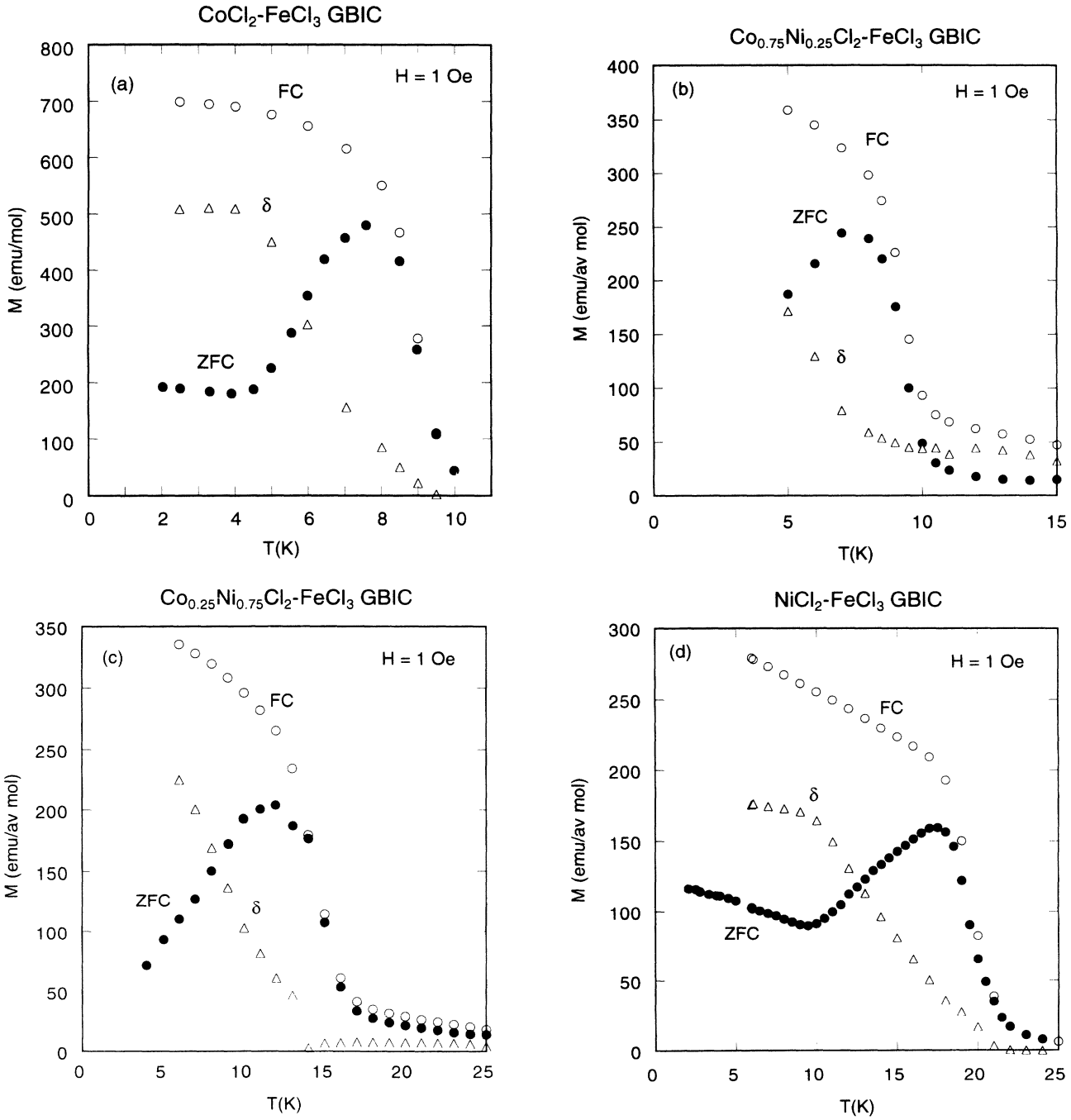

FIG. 8. Temperature variation of field-cooled magnetization M_{FC} (○), zero-field-cooled magnetization M_{ZFC} (●), and δ ($=M_{FC}-M_{ZFC}$) (△) for $Co_cNi_{1-c}Cl_2$-$FeCl_3$ GBIC's with (a) $c=1$, (b) 0.75, (c) 0.25, and (d) 0, where $H=1$ Oe and $\mathbf{H}\perp\mathbf{c}$.

Figure 9 shows the field dependence of SQUID magnetization M for $CoCl_2$-$FeCl_3$ GBIC at $T=2.5$ and 6 K when H was increased from 1 Oe to 1 kOe.[25] The following procedure was done before the measurement: (i) the sample was cooled from 300 to 2.5 K at $H=0$ in 5 min, (ii) H was increased from 0 to 50 kOe at 2.5 K ($M=1.54\times10^4$ emu/av mol at $T=2.5$ K and $H=50$ kOe), and (iii) H was decreased from 50 kOe to 1 Oe. As shown in Fig. 9 the value of M at 2.5 K is much larger than that at 6 K for $H\ll H_c(\approx40$ Oe) and is almost the same as that at 6 K for $H>H_c$. The field H_c corresponds to the spin-flop field for the antiferromagnetic phase of stage-2 $CoCl_2$ GIC,[26] where the 2D ferromagnetic layers are antiferromagnetically stacked along the c axis. In Sec. V C this increase of M at 2.5 K will be discussed in terms of the spin-frustration effect arising from a competition between the interplanar interaction between the $Co_cNi_{1-c}Cl_2$ and the $FeCl_3$ layers, and the intraplanar antiferromagnetic interaction in the $FeCl_3$ layer. We will show that the increase of M at 2.5 K gives an evidence that the $FeCl_3$ layers are antiferromagnetically ordered below T_N.

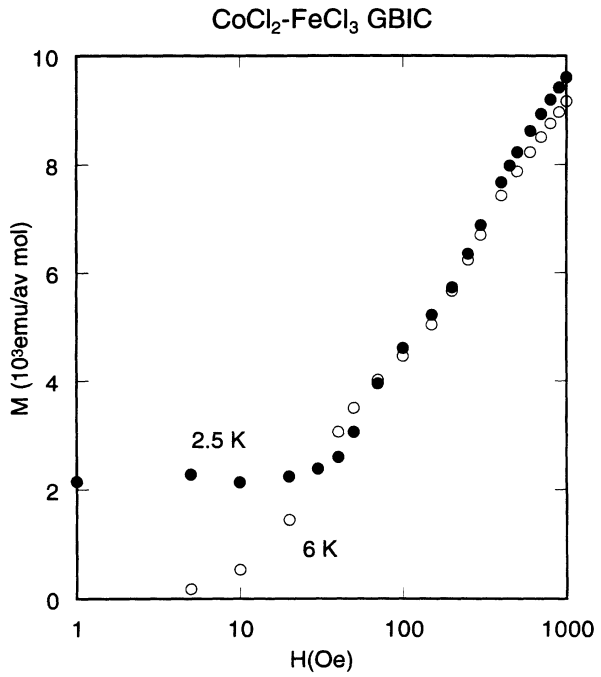

FIG. 9. Magnetic-field dependence of SQUID magnetization M for $CoCl_2$-$FeCl_3$ GBIC at $T=2.5$ K (●) and 6 K (○), where H⊥c.

V. DISCUSSION

A. Curie-Weiss temperature and effective magnetic moment

First we discuss the magnetic properties of $Co_cNi_{1-c}Cl_2$-$FeCl_3$ GBIC's at high temperatures where the dc magnetic susceptibility obeys the Curie-Wiess law. The concentration dependence of the effective magnetic moment and Curie-Weiss temperature for $Co_cNi_{1-c}Cl_2$-$FeCl_3$ GBIC's shown in Figs. 3 and 4 is compared with the prediction from the molecular field theory.[5] The effective magnetic moment $P_{\rm eff}$(GBIC) of $Co_cNi_{1-c}Cl_2$-$FeCl_3$ GBIC's with the stoichiometry $C_n(Co_cNi_{1-c}Cl_2)_{1-b}(FeCl_3)_b$ is predicted from this theory as

$$P_{\rm eff}({\rm GBIC})=[bP^2_{\rm eff}({\rm Fe})+(1-b)P^2_{\rm eff}({\rm RMGIC})]^{1/2}\ , \quad (5)$$

with

$$P_{\rm eff}({\rm RMGIC})=[cP^2_{\rm eff}({\rm Co})+(1-c)P^2_{\rm eff}({\rm Ni})]^{1/2}\ , \quad (6)$$

where $P_{\rm eff}$(RMGIC) is the effective magnetic moment (per average atom) of stage-2 $Co_cNi_{1-c}Cl_2$ GIC's. Here we use $P_{\rm eff}$(Fe) for stage-2 $FeCl_3$ GIC, $P_{\rm eff}$(Co) for stage-2 $CoCl_2$ GIC, and $P_{\rm eff}$(Ni) for stage-2 $NiCl_2$ GIC: $P_{\rm eff}({\rm Fe})=6.57\mu_B$, $P_{\rm eff}({\rm Co})=5.54\mu_B$, and $P_{\rm eff}({\rm Ni})=3.29\mu_B$.[4–6] In Fig. 3 the relation of $P_{\rm eff}$ vs c derived from Eq. (5) is denoted by a solid line for $b=0$, a dashed line for $b=0.3$, and a dotted line for $b=0.4$. Note that $b\approx0.4$ for the ideal stoichiometry of $Co_cNi_{1-c}Cl_2$-$FeCl_3$ GBIC's as described in Sec. IV A. The data of $P_{\rm eff}$ vs c for stage-2 $Co_cNi_{1-c}Cl_2$ GIC's fit well with the solid line with $b=0$. The data of $P_{\rm eff}$ vs c for $Co_cNi_{1-c}Cl_2$-$FeCl_3$ GBIC's lie roughly between the dashed line with $b=0.3$ and the dotted line with $b=0.4$ in the concentration range $0.2\le c\le0.8$. This result indicates that the stoichiometry of our GBIC samples is close to that of ideal GBIC's. A deviation of $P_{\rm eff}$ from the dashed line with $b=0.3$ to the solid line with $b=0$ is observed for $c<0.1$ and $c>0.8$. The value of $P_{\rm eff}$ for $CoCl_2$-$FeCl_3$ GBIC is almost the same as that of stage-2 $CoCl_2$ GIC, suggesting that the value of b is smaller than that derived from the weight-uptake measurement ($b=0.37$).

The Curie-Weiss temperatures Θ(GBIC) for $Co_cNi_{1-c}Cl_2$-$FeCl_3$ GBIC's can be predicted from the molecular field theory[5] as

$$P^2_{\rm eff}({\rm GBIC})\Theta({\rm GBIC})=(1-b)P^2_{\rm eff}({\rm RMGIC})\Theta({\rm RMGIC})+bP^2_{\rm eff}({\rm Fe})\Theta({\rm Fe})\ , \quad (7)$$

with

$$P^2_{\rm eff}({\rm RMGIC})\Theta({\rm RMGIC})=c^2P^2_{\rm eff}({\rm Co})\Theta({\rm Co})+(1-c)^2P^2_{\rm eff}({\rm Ni})\Theta({\rm Ni})+2c(1-c)\frac{J({\rm Co\text{-}Ni})}{\sqrt{|J({\rm Co\text{-}Co})J({\rm Ni\text{-}Ni})|}}P_{\rm eff}({\rm Co})P_{\rm eff}({\rm Ni})\sqrt{|\Theta({\rm Co})\Theta({\rm Ni})|}\ , \quad (8)$$

where Θ(RMGIC) is the Curie-Weiss temperature for stage-2 $Co_cNi_{1-c}Cl_2$ GIC's. We note that Θ(GBIC) coincides with Θ(RMGIC) for $b=0$. In Eq. (7) we assume that the interplanar interaction between the $Co_cNi_{1-c}Cl_2$ layer and the $FeCl_3$ layer is extremely weak compared with the intraplanar exchange interactions in $Co_cNi_{1-c}Cl_2$ layers and $FeCl_3$ layers. Here we use Θ(Fe) for stage-2 $FeCl_3$ GIC, Θ(Co) for stage-2 $CoCl_2$ GIC, and

Θ(Ni) for stage-2 $NiCl_2$ GIC: Θ(Fe)$=-4.3$ K, Θ(Co)$=23.2$ K, and Θ(Ni)$=70.0$ K. The intraplanar exchange interaction between Co and Ni is assumed to be 9.88 K.[5]

We calculate the value of Θ as a function of concentration c using Eq. (7). The results of numerical calculations for Θ vs c are shown in Fig. 4 for various values of b ($b=0$, 0.1, 0.2, and 0.3). We find that the data of Θ vs c for stage-2 $Co_cNi_{1-c}Cl_2$ GIC's denoted by open circles agree well with the broken line ($b=0$). On the other hand, the data of Θ vs c for $Co_cNi_{1-c}Cl_2$-$FeCl_3$ GBIC's lie between the dash dotted line ($b=0.1$) and solid line ($b=0.2$), indicating a smaller value of b. We think that the values of b determined from the weight-uptake measurement and the data of $P_{\rm eff}$ vs c is more precise than that determined from the data Θ vs c. We take the values of J(Co-Co), J(Ni-Ni), and J(Fe-Fe) for the stage-2 $CoCl_2$ GIC, stage-2 $NiCl_2$ GIC, and stage-2 $FeCl_3$ GIC in our calculation of Θ vs c. The intraplanar exchange interactions of GBIC's are considered to be different from those of GIC's. By an appropriate choice of Θ(Co), Θ(Ni), and Θ(Fe) for GBIC's our data of Θ vs c agree well with Eq. (7) with $b=0.37$. Note that the exact values of Θ(Co), Θ(Ni), and Θ(Fe) for GBIC's cannot be determined because of b being different for samples as listed in Table I.

B. Cluster-glass phase

Next we discuss the magnetic phase transition of $Co_cNi_{1-c}Cl_2$-$FeCl_3$ GBIC's near T_c. As described in Sec. IV D, the cluster-glass phase occurs below T_c for $Co_cNi_{1-c}Cl_2$-$FeCl_3$ GBIC's. The nature of this cluster-glass phase is described as follows. The $Co_cNi_{1-c}Cl_2$-$FeCl_3$ GBIC's belong to acceptor-type GIC's where a charge transfer occurs from graphite layers to intercalate layers. The $Co_cNi_{1-c}Cl_2$ layers are assumed to be formed of small islands whose diameter is on the order of 500 Å. The periphery of small islands provides acceptor sites for electrons transferred from graphite layers to $Co_cNi_{1-c}Cl_2$ layers. The spins within each island of $Co_cNi_{1-c}Cl_2$ layers are ferromagnetically ordered below T_c, forming a ferromagnetic cluster. The spin directions of Co^{2+} and Ni^{2+} lie in the c plane due to the XY spin anisotropy. The spin directions of these ferromagnetic clusters are frozen because of frustrated interisland interactions[24] consisting of both the dipole-dipole interaction between ferromagnetic clusters and interplanar exchange interaction between adjacent $Co_cNi_{1-c}Cl_2$ layers. This interplanar exchange interaction between adjacent $Co_cNi_{1-c}Cl_2$ layers should be enhanced by the intervening $FeCl_3$ layers through the interplanar interaction between $Co_cNi_{1-c}Cl_2$ and $FeCl_3$ layers which will be discussed in Sec. V C. The broad peak of $M_{\rm ZFC}$ results from a competition between thermal energy and these frustrated interisland interactions. In the temperature range $T_{\max}<T<T_c$, the spins within each island are still ferromagnetically aligned, but the spin directions of these ferromagnetic clusters become random because the thermal energy overcomes the frustrated interisland interaction around $T_{\max}$. For $T>T_c$ the system enters into the paramagnetic phase where spins within each island become random.

Just below T_c where the existence of $FeCl_3$ layers has no significant effect on the magnetic properties of $Co_cNi_{1-c}Cl_2$-$FeCl_3$ GBIC's, it is expected that like stage-2 $CoCl_2$ GIC and stage-2 $NiCl_2$ GIC the spins of ferromagnetic clusters in one $Co_cNi_{1-c}Cl_2$ layer of $Co_cNi_{1-c}Cl_2$-$FeCl_3$ GBIC's are antiferromagnetically coupled to those in the nearest-neighbor $Co_cNi_{1-c}Cl_2$ layer by an effective interplanar exchange interaction

$$J'_{\rm eff}(M-M)=\frac{2\pi}{\sqrt{3}}\left[\frac{\xi_M}{a_M}\right]^2 J'(M-M)\ , \tag{9}$$

where $J'(M-M)$ is an antiferromagnetic interplanar exchange interaction between M^{2+} spins of adjacent $Co_cNi_{1-c}Cl_2$ layers, and ξ_M is the in-plane spin correlation length of the $Co_cNi_{1-c}Cl_2$ layers. The value of ξ_M becomes large with decreasing temperature and is considered to be larger than the island size below T_c.

C. Interplanar interaction

Finally we discuss the effect of interplanar interaction between $Co_cNi_{1-c}Cl_2$ layers and $FeCl_3$ layers on the magnetic properties of $Co_cNi_{1-c}Cl_2$-$FeCl_3$ GBIC's at low temperatures below T_c. In Sec. II B, it has been shown that for the stage-1 and stage-2 $FeCl_3$ GIC's the short-range spin order develops below 30 K in $FeCl_3$ layers. The magnetic Bragg peak is observed at the in-plane wave number $|\mathbf{Q}_\perp|=0.394\ |\mathbf{a}^+|$. The in-plane spin structure of $FeCl_3$ layers is different from a $\sqrt{3}\times\sqrt{3}$ (120°) spin structure predicted for a 2D XY antiferromagnet on the triangular lattice: $|\mathbf{Q}_\perp|=|\mathbf{a}^+|/\sqrt{3}$. One can expect that such a short-range order develops at temperatures far above T_N in the $FeCl_3$ layer of $Co_cNi_{1-c}Cl_2$-$FeCl_3$ GBIC's. This short-range order grows as the temperature decreases, and becomes an antiferromagnetic long-range order below T_N. Here we consider the effect of an interplanar interaction between $Co_cNi_{1-c}Cl_2$ and $FeCl_3$ layers on the spin order in the $FeCl_3$ layer. For further discussion we notice that the spin directions of Co^{2+}, Ni^{2+}, and Fe^{3+} spins lie in the c plane due to the XY spin anisotropy.

In the absence of an external magnetic field, just below T_c the ferromagnetically ordered $Co_cNi_{1-c}Cl_2$ layers are considered to be stacked antiferromagnetically along the c axis irrespective of the nature of the interplanar interaction between $Co_cNi_{1-c}Cl_2$ and $FeCl_3$ layers. The direction of spins in one $Co_cNi_{1-c}Cl_2$ layer is antiparallel to those in the adjacent $Co_cNi_{1-c}Cl_2$ layer. Thus the molecular field acting on the $FeCl_3$ layer from one $Co_cNi_{1-c}Cl_2$ layer is canceled out by that from the adjacent $Co_cNi_{1-c}Cl_2$ layer, implying that the interplanar interaction has no effect on the spin order of $FeCl_3$ layers. When the magnetic field, which is larger than a spin-flop field $H_0(\approx 40$ Oe), is applied along any direction perpendicular to the c axis, the spins in the $Co_cNi_{1-c}Cl_2$ layers tend to align along the field direction, forming the ferromagnetic spin alignment of the $Co_cNi_{1-c}Cl_2$ layers

along the c axis. The molecular field acting on the $FeCl_3$ layer by one $Co_cNi_{1-c}Cl_2$ layer is parallel to that from the adjacent $Co_cNi_{1-c}Cl_2$ layer. When the interplanar interaction between $Co_cNi_{1-c}Cl_2$ and $FeCl_3$ layers is antiferromagnetic, the resultant molecular field on the $FeCl_3$ layer is antiparallel to the field direction.

The interplanar interaction between the $Co_cNi_{1-c}Cl_2$ and the $FeCl_3$ layers is considered to consist of dipole-dipole interaction and interplanar exchange interaction. The dipole-dipole interaction between the spin vector ($=\mathbf{S}_M$) in the $Co_cNi_{1-c}Cl_2$ layer and Fe^{3+} spin vector ($=\mathbf{S}_{Fe}$) can be described by

$$H=\frac{g_M g_{Fe}\mu_B^2}{r^3}\left\{\mathbf{S}_M\cdot\mathbf{S}_{Fe}-\frac{3(\mathbf{S}_M\cdot\mathbf{r})(\mathbf{S}_{Fe}\cdot\mathbf{r})}{r^2}\right\}, \quad (10)$$

where g is the Landé g factor and $\mathbf{r}$ is a position vector connecting between two sites and is along the c axis: $r\approx 9.35$ Å. Since the directions of $\mathbf{S}_M$ and $\mathbf{S}_{Fe}$ are perpendicular to the c axis, the dipole-dipole interaction can be rewritten as

$$H=\left[\frac{g_M g_{Fe}\mu_B^2}{r^3}\right]\mathbf{S}_M\cdot\mathbf{S}_{Fe}=-2U_0\mathbf{S}_M\cdot\mathbf{S}_{Fe}, \quad (11)$$

implying that this dipole-dipole interaction is energetically favorable for the antiparallel spin alignment for $\mathbf{S}_M$ and $\mathbf{S}_{Fe}$. The value of U_0 is estimated as $U_0=-1.8\times10^{-3}$ K for $NiCl_2$-$FeCl_3$ GBIC: $g_{Ni}=2.33$, $g_{Fe}\approx 2$. The interaction U_0 is extremely weak compared with that of the intraplanar exchange interactions: J(Co-Co)=7.75 K, J(Ni-Ni)=8.75 K, J(Co-Ni)=9.88 K, and J(Fe-Fe)=−0.34 K. In order to explain the magnetization data of $Co_cNi_{1-c}Cl_2$-$FeCl_3$ GBIC's shown in Fig. 6(b), the interplanar interaction between the $Co_cNi_{1-c}Cl_2$ and the $FeCl_3$ layers should be antiferromagnetic. The interplanar interaction can be described by $H=-2J'(M-\text{Fe})\mathbf{S}_M\cdot\mathbf{S}_{Fe}$, where $J'(M$-Fe) (<0) is an antiferromagnetic interplanar interaction between a M spin in the $Co_cNi_{1-c}Cl_2$ layer and a Fe^{3+} spin in the $FeCl_3$ layer, and is given by the sum of the dipole-dipole interaction constant U_0 and the interplanar exchange interaction.

In the temperature range between T_c and T_N, the spins in the $Co_cNi_{1-c}Cl_2$ layers form ferromagnetic clusters, while the spins in the $FeCl_3$ layer are correlated with each other within the distance of the in-plane spin correlation length ξ_{Fe}. This distance ξ_{Fe} is assumed to be smaller than the size of a ferromagnetic cluster. Furthermore, if there is no interplanar interaction between $Co_cNi_{1-c}Cl_2$ and $FeCl_3$ layers, the Fe^{3+} spins within the distance ξ_{Fe} are assumed to be aligned to the field direction because of the Zeeman energy overcoming the weak antiferromagnetic intraplanar exchange interactions. Then the effective interplanar interaction $J'_{eff}(M$-Fe) is approximately given by

$$J'_{eff}(M\text{-}Fe)=\frac{4\pi}{\sqrt{3}}\left[\frac{\xi_{Fe}}{a_{Fe}}\right]^2 J'(M\text{-Fe}) . \quad (12)$$

Because of $J'_{eff}(M$-Fe), which becomes more significant below T_c, Fe^{3+} spins are focused to be aligned in the direction antiparallel to the field direction, leading to a drastic decrease of the magnetization. In fact, as shown in Fig. 6(b), the value of χ_{max} for $Co_cNi_{1-c}Cl_2$-$FeCl_3$ GBIC's is much smaller than that for stage-2 $Co_cNi_{1-c}Cl_2$ GIC's with the same concentration c.

Below T_N the $FeCl_3$ layers are antiferromagnetically ordered: the Fe^{3+} spins are considered to be strongly coupled through the intraplanar antiferromagnetic interaction in the $FeCl_3$ layers. The effective interplanar interaction $J'_{eff}(M$-Fe) forces the Fe^{3+} spins to be antiparallel to the ferromagnetic spins in the $Co_cNi_{1-c}Cl_2$ layers. Then the spin-frustration effect is considered to occur in the $FeCl_3$ layers as a result of a competition between $J'_{eff}(M$-Fe) and antiferromagnetic intraplanar interaction between Fe^{3+} spins. Due to this spin-frustration effect, the directions of Fe^{3+} spins are no longer antiparallel to the field direction, leading to an increase of the magnetization along the field direction. As shown in Fig. 9, the magnetization of $CoCl_2$-$FeCl_3$ GBIC at 2.5 K ($<T_N$) is larger than that at 6 K for $1<H<40$ Oe. In terms of our model we can explain that (i) the magnetization at 2.5 K should be larger than that at 6 K for $H>H_c$ and that (ii) the magnetization at 6 K is almost equal to zero for $H<H_c$. The finite value of M at 2.5 K for $H\ll H_c$ may be due to several effects including the spin-frustration effect described above and the antiferromagnetic interplanar exchange interaction between adjacent $CoCl_2$ layers.

VI. CONCLUSION

The magnetic properties of $Co_cNi_{1-c}Cl_2$-$FeCl_3$ GBIC's with a stacking sequence of -G-$Co_cNi_{1-c}Cl_2$-G-$FeCl_3$-G- along the c axis have been studied and compared with those of stage-2 $Co_cNi_{1-c}Cl_2$ GIC's with the c-axis stacking sequence of -G-$Co_cNi_{1-c}Cl_2$-G-G-Co_cNi_{1-c}-G- . The $Co_cNi_{1-c}Cl_2$-$FeCl_3$ GBIC's undergo a magnetic phase transition at the critical temperature T_c, below which a cluster-glass phase appears. The spin directions of ferromagnetic clusters in the $Co_cNi_{1-c}Cl_2$ layers are frozen because of the frustrated interisland interactions. The critical temperature T_c of $Co_cNi_{1-c}Cl_2$-$FeCl_3$ GBIC's is almost the same as that of stage-2 $Co_cNi_{1-c}Cl_2$ GIC's. The critical behavior of $Co_cNi_{1-c}Cl_2$-$FeCl_3$ GBIC's near T_c is 3D XY-like due to the intervening $FeCl_3$ layer, while the critical behavior of stage-2 $Co_cNi_{1-c}Cl_2$ GIC's is 2D XY-like. Below T_N this cluster-glass phase may coexist with an antiferromagnetic long-range order occurring in the $FeCl_3$ layers. The effect of antiferromagnetic interplanar interaction between the $FeCl_3$ layer and the $Co_cNi_{1-c}Cl_2$ layer is clearly seen in the magnetization of $Co_cNi_{1-c}Cl_2$-$FeCl_3$ GBIC's. The nature of the coexisting phase below T_N is considered to be complicated because of the spin-frustration effect arising from the competition between the interplanar interaction between the $FeCl_3$ layer and the $Co_cNi_{1-c}Cl_2$ layer and the antiferromagnetically intraplanar interaction of the $FeCl_3$ layer. Further detailed study on the magnetic properties of these compounds at

low temperatures will be required for better understanding.

ACKNOWLEDGMENTS

We would like to thank H. Suematsu and Y. Hishiyama for providing us with high-quality single-crystal kish graphites, J. Sciorra, F. Khemai, J. Morillo, and N. Inadama for their help in the sample preparation of RMGIC's and GBIC's, and M. Johnson for his help in the dc magnetic-susceptibility measurement. The SQUID magnetization measurement was carried out when two of us (I.S.S. and M.S.) stayed at the Institute for Molecular Science in Japan. We are grateful to Y. Maruyama for giving us an opportunity to use the SQUID magnetometer. The work at SUNY at Binghamton was supported by NSF DMR-9201656, and the work at the Institute for Molecular Science was supported by Grant-in-Aid for Scientific Research from the Ministry of Education, Science, and Culture of Japan 04NP0301.

[1]S. A. Solin and H. Zabel, Adv. Phys. **37**, 87 (1988).

[2]P. Lagrange and R. Setton, *Graphite Intercalation Compounds 1, Structure and Dynamics,* edited by H. Zabel and S. A. Solin (Springer-Verlag, New York, 1990), p. 283.

[3]R. Setton, *Graphite Intercalation Compounds 1, Structure and Dynamics,* edited by H. Zabel and S. A. Solin (Springer-Verlag, New York, 1990), p. 305.

[4]M. Yeh, M. Suzuki, and C. R. Burr, Phys. Rev. B **40**, 1422 (1989).

[5]M. Yeh, I. S. Suzuki, M. Suzuki, and C. R. Burr, J. Phys. Condens. Matter **2**, 9821 (1990).

[6]M. Suzuki, I. S. Suzuki, W. Zhang, F. Khemai, and C. R. Burr, Phys. Rev. B **46**, 5311 (1992).

[7]I. S. Suzuki, M. Suzuki, L. F. Tien, and C. R. Burr, Phys. Rev. B **43**, 6393 (1991).

[8]I. S. Suzuki and M. Suzuki, J. Phys. Condens. Matter **3**, 8825 (1991).

[9]I. S. Suzuki, F. Khemai, M. Suzuki, and C. R. Burr, Phys. Rev. B **45**, 4721 (1992).

[10]M. Suzuki, I. S. Suzuki, M. Johnson, J. Morrilo, and C. R. Burr, Phys. Rev. B **50**, 204 (1994).

[11]J. T. Nicholls and G. Dresselhaus, Phys. Rev. B **41**, 9744 (1990).

[12]I. S. Suzuki, C.-J. Hsieh, F. Khemai, C. R. Burr, and M. Suzuki, Phys. Rev. B **47**, 845 (1993).

[13]M. Suzuki, I. Oguro, and Y. Jinzaki, J. Phys. C **17**, L575 (1984).

[14]D. G. Rancourt, B. Hun, and S. Flandrois, Ann. Phys. (Paris) **11**, Colloq. No. 2, Suppl. No. 2 107 (1986).

[15]D. G. Rancourt, B. Hun, and S. Flandrois, Can. J. Phys. **66**, 776 (1988).

[16]I. Rosenman, F. Batallan, Ch. Simon, and L. Hachim, J. Phys. (Paris) **47**, 1221 (1986).

[17]S. Chehab, P. Biensan, J. Amiell, and S. Flandrois, J. Phys. (France) I **1**, 537 (1991).

[18]S. Chehab, P. Biensan, S. Flandrois, and J. Amiell, Phys. Rev. B **45**, 2844 (1992).

[19]K. Ohhashi and I. Tsujikawa, J. Phys. Soc. Jpn. **36**, 980 (1974).

[20]Ch. Simon, F. Batallan, I. Rosenman, J. Schweitzer, H. Lauter, and R. Vangelisti, J. Phys. (Paris) Lett. **44**, L641 (1983).

[21]Ch. Simon, F. Batallan, I. Rosenman, G. Furdin, R. Vangelisti, H. Lauter, J. Schweitzer, C. Ayache, and G. Pepy, Ann. Phys. (Paris) Colloq. No. 2, Suppl. No. 2, **11**, 143 (1986).

[22]J. S. Speck, J. T. Nicholls, B. J. Wuensch, J. M. Delgado, M. S. Dresselhaus, and H. Miyazaki, Philos. Mag. B **64**, 181 (1991).

[23]See, for example, M. F. Collins, *Magnetic Critical Scattering* (Oxford Universtiy, New York, 1989), p. 29.

[24]I. S. Suzuki, M. Suzuki, and Y. Maruyama, Phys. Rev. B **48**, 13 550 (1993).

[25]M. Suzuki, I. S. Suzuki, C. Vartuli, C. R. Burr, and Y. Maruyama, Mol. Cryst. Liq. Cryst. **245**, 93 (1994).

[26]M. Suzuki, Crit. Rev. Solid State Mater. Sci. **16**, 237 (1990).